Biochemistry

 Volume 14, Number 19 September 23, 1975

# Mössbauer Investigations of High-Spin Ferrous Heme Proteins. I. Cytochrome P-450†

P. M. Champion,‡ J. D. Lipscomb,§ E. Münck,§ P. Debrunner,* and I. C. Gunsalus

ABSTRACT: Anaerobically reduced samples of cytochrome P-450 from *Pseudomonas putida* were studied by Mössbauer spectroscopy. In the presence of an applied magnetic field the high-spin ferrous heme iron showed an intricate pattern of electric and magnetic hyperfine interactions which could be parametrized successfully in terms of a spin Hamiltonian formalism. The results imply a very low (triclinic) symmetry of the heme iron. The effects of the ligand environment and of spin–orbit coupling result in a large zero-field splitting of the electronic ground state. The electric-field gradient tensor is characterized by a large asymmetry parameter, and its principal axes are rotated substantially from the frame that defines the zero-field splitting. This study shows that high-field Mössbauer spectroscopy provides a unique tool for structural investigations of high-spin ferrous compounds and can substitute, under suitable conditions, for magnetic susceptibility measurements. The present paper focuses on the methodology and data analysis; in the subsequent paper the data obtained for P-450 are compared with new results obtained for hemoglobin, chloroperoxidase, and horseradish peroxidase.

Cytochromes of the P-450 type were first identified in liver microsomes on the basis of the characteristic Soret absorption near 450 nm that they exhibit upon reduction and complexation with CO (Klingenberg, 1958; Garfinkel, 1958). These cytochromes demonstrated monoxygenase activity toward many drugs, steroid hormones, polycyclic compounds, and a variety of other potentially toxic molecules. Other important P-450 cytochromes, in particular those from the adrenal cortex mitochrondria, are involved in steroid metabolism (Schleyer et al., 1972). All the mammalian cytochromes P-450 are membrane bound, and only recently has it been possible to solubilize them in active, homogeneous form (Imai and Sato, 1974; van der Hoeven et al., 1974). Gunsalus and coworkers, however, found a soluble cytochrome P-450 in the camphor hydroxylase from *Pseudomonas putida* (Hedegaard and Gunsalus, 1965). This three-component enzyme system closely resembles the adrenocortical hydroxylase (Schleyer et al., 1972) and, because of its solubility and easy accessibility, provides an ideal model for the mammalian monoxygenases. A comprehensive summary of the chemical and physical properties of this enzyme system, in particular of the stable intermediate states of cytochrome P-450, was given by Gunsalus et al. (1974).

Spectroscopically, cytochrome P-450 differs in many respects from a typical heme protein such as hemoglobin, and several authors have speculated on the nature and the geometry of the heme ligands that might be responsible for these differences (Bayer et al., 1969; Stern et al., 1973; Stern and Peisach, 1974). Whereas the oxidized states of cytochrome P-450 have been studied in detail by electron paramagnetic resonance (EPR) and Mössbauer spectroscopy (Gunsalus et al., 1974), relatively little is known about the reduced state of the enzyme. $^{57}$Fe-Mössbauer spectroscopy can fill this gap, since it applies to all charge and spin states of iron, including the EPR-silent ferrous state. It measures the internal electric and magnetic fields acting on the nucleus and yields detailed information about the electronic ground state of the heme iron.

An earlier Mössbauer study of reduced camphor-complexed cytochrome P-450 revealed a quadrupole splitting and an isomer shift characteristic of high-spin ferrous iron (Sharrock et al., 1973). In this respect it is an analog of deoxyhemoglobin and, like the latter, reversibly binds small molecules such as $O_2$, CO, and NO. In spite of this similarity, there are substantial differences between the electronic ground states of the two proteins. The quadrupole splitting of hemoglobin is strongly temperature dependent; several authors (Huynh et al., 1974; Trautwein et al., 1970) conclude from a crystal field model that excited singlet and triplet states may be populated near room temperature in addition to the quintet ground state. Reduced cytochrome

† From the Departments of Physics and Biochemistry, University of Illinois at Urbana—Champaign, Urbana, Illinois 61801. *Received April 1, 1975.* Supported in part by grants from the U.S. Public Health Service, GM 16406 and AM562-22.

‡ Present address: Laboratory of Atomic and Solid State Physics, Cornell University, Ithaca, New York 14850.

§ Present address: Freshwater Biological Institute, University of Minnesota, Navarre, Minnesota 55392.

P-450, on the other hand, has an almost temperature independent quadrupole splitting, and only the five spin states of the orbitally nondegenerate ground state are expected to be populated. Substantial differences in the zero-field splitting $D$ of the lowest quintet have been derived from magnetic susceptibility data. Champion et al. (1975a) obtained $D \approx 20$ K for cytochrome P-450, in agreement with Mössbauer experiments, whereas Nakano et al. (1971, 1972) inferred a value of $D = 7.5$ K for deoxyhemoglobin; however, all states other than the lowest quintet were ignored.

The present paper examines the Mössbauer spectra of high-spin ferrous P-450 in detail, while the subsequent paper (Champion et al., 1975c) extends the discussion to three other heme proteins. We show that the spectra of P-450 observed in a strong magnetic field consist of an intricate pattern of electric and magnetic hyperfine interactions which have been parametrized successfully in a spin Hamiltonian formalism. To our knowledge these are the first well-resolved magnetically split Mössbauer spectra of a high-spin ferrous heme protein. In the next section we discuss the spin Hamiltonian formalism and its application to Mössbauer experiments in external magnetic fields. Two limiting cases are then briefly considered, low-temperature, low-field spectra and high-temperature, high-field spectra. Both cases are experimentally very useful since they allow the independent determination of some of the parameters in the spin Hamiltonian. Following the experimental procedure the results are presented, and a final section is devoted to the discussion.

## Theory

In order to lay the ground work for the detailed presentation of the paramagnetic Mössbauer spectra that follows, we turn to a spin Hamiltonian approximation that works very well in describing the data. Johnson (1967) successfully applied this formalism to describe high-field Mössbauer spectra of ferrous fluosilicate. Presently, spin Hamiltonian parameters do not lend themselves to a straightforward interpretation of molecular structure. Nevertheless such a description of the data is of considerable value since it allows the experimental data to be parametrized in a compact fashion and permits systematic comparison of the results for various heme proteins.

The pertinent spin Hamiltonian describing the Mössbauer spectra of the ferrous ion depends on electronic and nuclear variables. The electronic part takes into account the zero-field splitting and the Zeeman interaction of the electronic ground state, which is a spin quintet ($S = 2$). The nuclear part describes the magnetic hyperfine interaction, the electric quadrupole interaction, and the nuclear Zeeman effect. The electronic part of the spin Hamiltonian may be written as

$$\mathcal{H} = D\{S_z^2 - 2 + (E/D)(S_x^2 - S_y^2)\} + \beta \mathbf{S}\cdot\tilde{\mathbf{g}}\cdot\mathbf{H} \quad (1)$$

where $D$ and $E$ are coefficients describing the splitting of the spin quintet in zero magnetic field. For heme proteins the two terms quadratic in $S$ yield energy splittings of the order of 1–50 $cm^{-1}$; other terms that may exist (Abragam and Bleaney, 1970), including those of fourth order in $S$, have been ignored since they are likely to be small in comparison with $D$ and $E$. Although eq 1 depends on electronic parameters only, both terms have a profound influence on the Mössbauer spectrum when the samples are studied in an applied field $\mathbf{H}$. The zero-field splitting lifts the fivefold spin degeneracy of the orbital ground state and the resulting eigenstates $|N\rangle$, $N = 1 \ldots 5$, are spin singlets, except when $E = 0$. In the absence of an applied field these singlet states have no magnetic moment, i.e., the expectation value of the electronic spin vanishes, $\langle \mathbf{S} \rangle_N = 0$. An applied magnetic field, however, mixes the states and produces a spin polarization, $\langle \mathbf{S} \rangle_N \neq 0$.

The magnetic hyperfine interaction is given by $\langle \mathbf{S} \rangle \cdot \tilde{\mathbf{A}} \cdot \mathbf{I}$, where $\tilde{\mathbf{A}}$ is the magnetic hyperfine tensor. The nuclear part of the Hamiltonian then is

$$\mathcal{H}_n = \langle \mathbf{S} \rangle \cdot \tilde{\mathbf{A}} \cdot \mathbf{I} - \mathbf{g}_n \beta_n \mathbf{H} \cdot \mathbf{I} + \mathcal{H}_Q \quad (2a)$$

with

$$\mathcal{H}_Q = (eQV_{\zeta\zeta}/12)[3I_\zeta^2 - 15/4 + \eta(I_\xi^2 - I_\eta^2)] \quad (2b)$$

for the excited ($I = 3/2$) nuclear state and $\mathcal{H}_Q = 0$ for the ground ($I = 1/2$) nuclear state. The form of the quadrupole interaction in eq 2 explicitly shows that the principal axes of the electric-field gradient tensor ($V_{\xi\xi}$, $V_{\eta\eta}$, $V_{\zeta\zeta}$) need not coincide with those of the zero-field splitting; $\eta = (V_{\xi\xi} - V_{\eta\eta})/V_{\zeta\zeta}$ is the asymmetry parameter (by convention $0 \leq \eta \leq 1$).

In the absence of an applied magnetic field, the spin expectation value $\langle \mathbf{S} \rangle$ vanishes and only the magnitude of the quadrupole splitting can be observed in polycrystalline samples, $|\Delta E_Q| = (eQV_{\zeta\zeta}/2)\sqrt{1 + 1/3\eta^2}$. Application of a strong magnetic field leads to a spin polarization, $\langle \mathbf{S} \rangle \neq 0$, and permits determination of all the quantities in eq 2.

We may rewrite eq 2a as

$$\mathcal{H}_n = -\mathbf{g}_n \beta_n [\mathbf{H} - \langle \mathbf{S} \rangle \cdot \tilde{\mathbf{A}}/(\mathbf{g}_n \beta_n)] \cdot \mathbf{I} + \mathcal{H}_Q \quad (3)$$

The quantity $\mathbf{H}_{int} = -\langle \mathbf{S} \rangle \cdot \tilde{\mathbf{A}}/(\mathbf{g}_n \beta_n)$, the internal magnetic field, determines the magnetic splittings of the nuclear ground and excited states. Since $\mathbf{H}_{int}$ depends on $\langle \mathbf{S} \rangle$ the electronic parameters introduced in eq 1 can be determined from Mössbauer measurements. Depending on the temperature $T$ and the electronic spin relaxation time four types of Mössbauer spectra can be expected.

(i) At temperatures such that $kT \ll D$ only the lowest spin state, $N = 1$, is populated, and the spin expectation value to be used in eq 2 and 3 is $\langle \mathbf{S} \rangle_1$, no matter whether the relaxation time is fast or slow. (ii) At higher temperatures, all five eigenstates $|N\rangle$ of eq 1 with energies $E_N$, $N = 1, \ldots 5$, have finite Boltzmann factors, $\exp(-E_N/kT)$, and the observed Mössbauer spectra then strongly depend on the spin relaxation time. For slow relaxation, a given molecule may exist in any of the five spin states predicted by eq 1, each giving rise to a different internal magnetic field $\mathbf{H}_{int}$. The resulting Mössbauer spectrum then is the weighted average of the spectral components from each individual eigenstate. (iii) For most high-spin ferrous compounds the electron spin relaxation time is fast compared to the nuclear precession times. The $^{57}Fe$ nucleus then sees a net expectation value of the electronic spin that is a thermal average, $\langle \mathbf{S} \rangle_T$, taken over the five spin states $|N\rangle$:

$$\langle \mathbf{S} \rangle_T = \left[ \sum_{N=1}^{5} \langle \mathbf{S} \rangle_N \exp(-E_N/kT) \right] \Big/ \left[ \sum_{N=1}^{5} \exp(-E_N/kT) \right] \quad (4)$$

As in case (i) each molecule has a well-defined internal magnetic field $\mathbf{H}_{int}$, but the spin expectation value to be used in eq 2 and 3 is now the thermal average, eq 4. (iv) For intermediate spin relaxation times the problem is more complicated, and no attempt is made in this paper to simulate Mössbauer spectra for this general case.

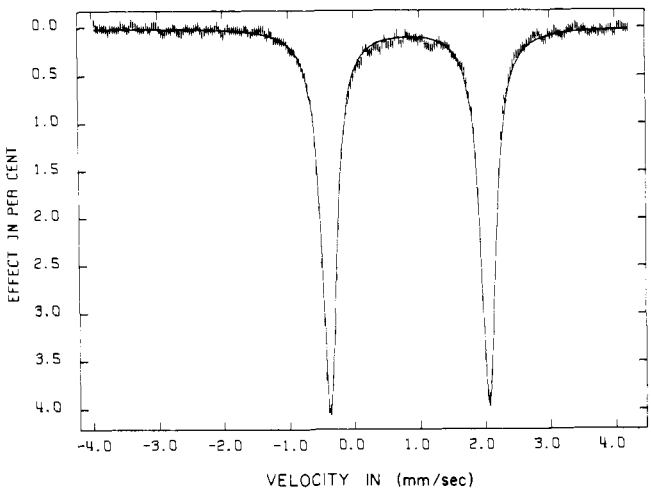


FIGURE 1: Mössbauer spectrum of reduced cytochrome P-450 taken in zero magnetic field at 4.2 K. The solid curve is the result of a least-squares fit to the data utilizing two Lorentzian lines of equal areas. The quadrupole splitting, $\Delta E_Q$, was found to be equal to 2.42 ± 0.03 mm/sec while the isomeric shift, $\delta$, was found to be 0.82 ± 0.02 mm/sec with respect to iron metal. The lack of absorption between 0 and 1.0 mm/sec indicates a magnetically "clean" sample. The narrow line width (FWHM) of 0.25 mm/sec implies that the sample is very homogeneous.

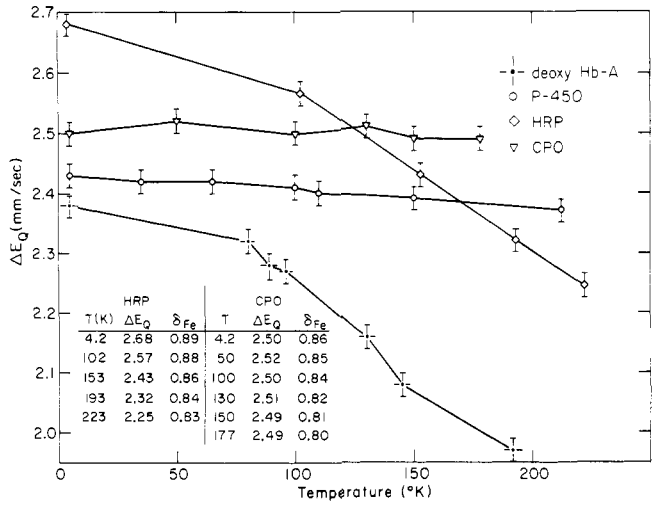


FIGURE 2: Quadrupole splitting $\Delta E_Q$ as a function of temperature for the four high-spin ferrous heme proteins deoxyhemoglobin (Huynh et al., 1974), cytochrome P-450 (Sharrock et al., 1975), horseradish peroxidase (HRP), and chloroperoxidase (CPO). The measured quadrupole splittings, $\Delta E_Q$, and isomer shifts, $\delta_{Fe}$, of ferrous HRP and CPO are listed in the insert. The values are given in units of Doppler shift (mm/sec) with an uncertainty of ±0.02 mm/sec. Isomer shifts are quoted relative to iron metal at 300 K.

The number of adjustable parameters in eq 1 and 2 is quite large and finding a reliable solution can be a formidable problem. There are three components apiece in the **A** and **g** tensors, two in the zero-field splitting and the electric-field gradient tensors, plus six Euler angles relating the principal axes systems of the **A** and EFG tensors to the frame defined by the zero-field splitting. The number of unknowns can be reduced, however, since the spectra are rather insensitive to the **g** tensor and since one can determine $\tilde{\mathbf{g}}$ via a simple second-order perturbation expansion (Zimmermann et al., 1974). Furthermore, for $D > 0$, it follows from eq 1 that $\langle S_z \rangle \approx 0$ for temperatures such that $kT$ is comparable to or smaller than the zero-field splitting; hence the Mössbauer spectra are insensitive to the component of the **A** tensor along the direction of $\langle S_z \rangle$. Moreover, by a judicious choice of experimental conditions the size of $\mathbf{H}_{int}$ can be controlled. Specifically, by measuring the spectra in fields of moderate strength ($g_n\beta_n\mathbf{H}_{int} < |\Delta E_Q|$) and at various temperatures ($T < 20$ K) we can independently estimate the magnitude of the zero-field splitting. Such measurements provide the same information as obtained from magnetic susceptibility data. In addition, such experiments give crucial information about the orientation of the electric-field gradient relative to the zero-field splitting. A detailed treatment of the methodology has been given by Champion (1975) and Champion et al. (1975b).

Finally, at higher temperatures ($(E_N - E_1)/kT \ll 1$) eq 4 yields the Curie law, i.e., $\mathbf{H}_{int} \sim 1/kT$. Thus at sufficiently high temperatures the internal magnetic field is small and the sample behaves like a diamagnet. Under these conditions the asymmetry parameter $\eta$ can be determined.

## Experimental Methods

The methods used for the purification and $^{57}$Fe enrichment of cytochrome P-450 from *Pseudomonas putida* have been described previously (Sharrock et al., 1973). The P-450 complex with substrate (camphor) was prepared under argon and reduced by dialysis against sodium dithionite. Samples with a P-450 concentration around 1 m*M* were frozen in small cylindrical nylon cups (1 ml) and stored under liquid nitrogen.

The Mössbauer spectrometer was of the constant acceleration type. A 45-mCi source of $^{57}$Co in rhodium was used, giving a minimum observable line width of 0.23 mm/sec (FWHM). The system was calibrated with a metallic iron absorber; all velocity scales and isomer shifts are referred to the iron standard. Variable temperature and weak magnetic field experiments were carried out with the sample placed in the tail section of a variable temperature dewar (Janis Research Co.), which allowed the placement of an electromagnet (Varian Model V-4004) around the sample. In this configuration, magnetic fields up to 6.6 kG could be generated. Sample temperatures between 1.5 and 200 K were easily obtained by the use of a small heating coil; they were monitored by means of calibrated 1/8-W carbon resistors or Keystone thermistors.

Experiments conducted in large applied magnetic fields (~45 kG) and at high temperatures (~200 K) were carried out in an Andonian dewar/superconducting magnet system with room temperature access. A simple liquid nitrogen heat exchanger was used to keep the temperature of the protein sample in the range between 160 and 200 K.

In order to carry out experiments in large magnetic fields and at low temperatures (4.2 or 1.6 K), we have designed and built a superconducting magnet with compensation coil. The achievement of acceptable field homogeneity presented no particular problem, since a field variation of up to 1% over the sample volume has negligible effect on the Mössbauer spectrum. The compensation coil allows the source to be placed about 3 cm from the sample, resulting in high count rates. The cryogenic system, housing this arrangement, is described in detail elsewhere (Champion, 1975).

## Results and Analysis

A typical Mössbauer spectrum of reduced cytochrome P-450, taken at 4.2 K in zero magnetic field, is shown in Figure 1; a symmetric quadrupole doublet with narrow absorption lines (0.23 mm/sec full width at half-maximum) is

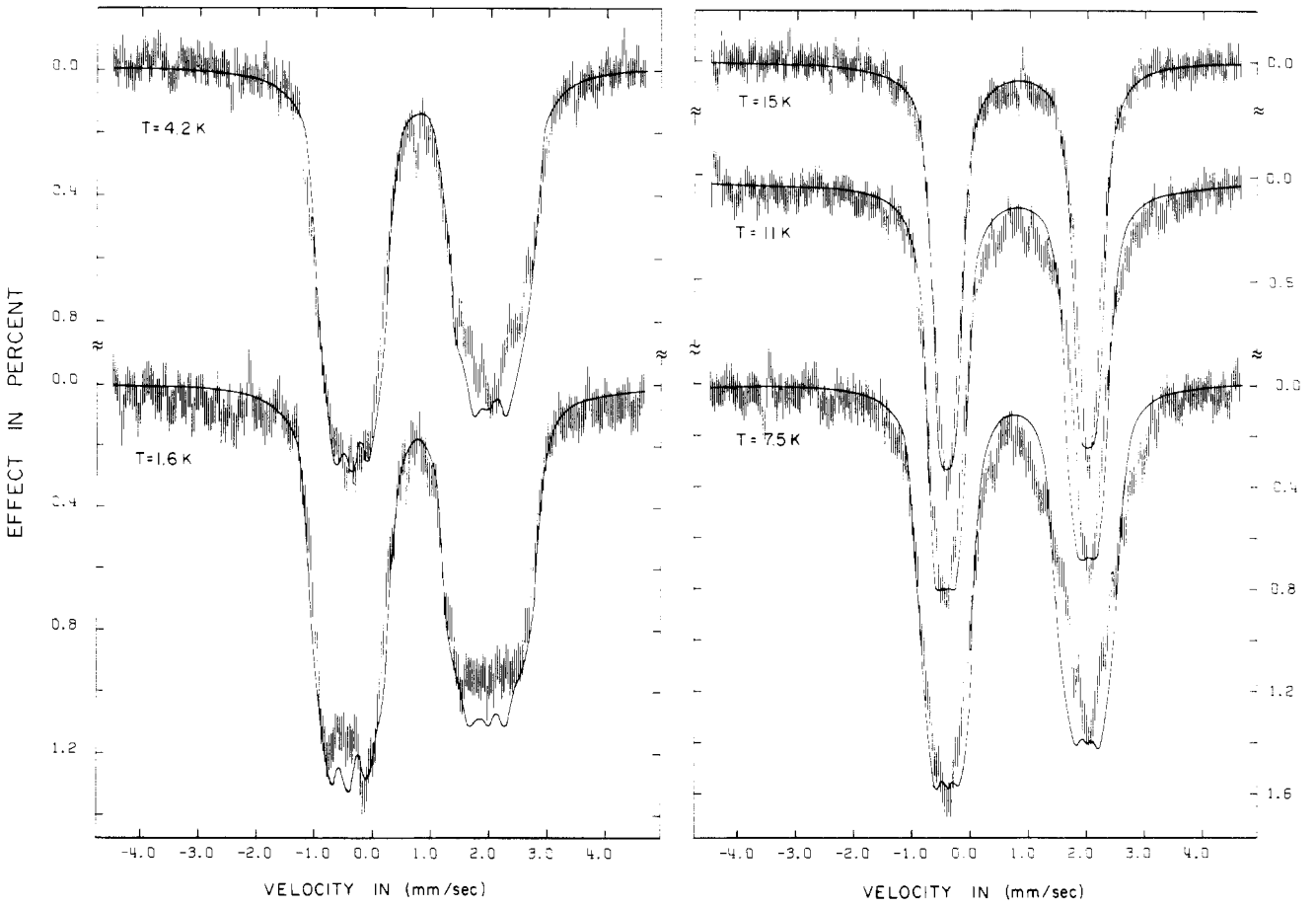


FIGURE 3: Mössbauer spectra of reduced P-450 taken in a 6.6-kG magnetic field applied perpendicular to the incident $\gamma$ radiation. The sample temperature is indicated beside each spectrum. The solid curves are the result of computer simulations using the parameters listed in Table I and assuming fast relaxation.

observed. The quadrupole splitting is almost independent of temperature (Figure 2) indicating an isolated orbital ground state, well separated in energy from the next orbital state. For comparison we have plotted in Figure 2 the quadrupole splittings for chloroperoxidase, horseradish peroxidase, and hemoglobin. The latter proteins will be discussed in paper II (Champion et al., 1975c).

As mentioned above, application of a strong magnetic field yields a polarization of the electronic spin resulting in Mössbauer spectra showing paramagnetic hyperfine structure. Figure 3 shows a series of spectra taken in a field of 6.6 kG, applied transverse to the observed Mössbauer radiation. The spectrum in Figure 4 was taken at 4.2 K in a 8.6-kG parallel field. Notice that the quadrupole splitting remains dominant, although the magnetic splitting, essentially due to the term $\langle \mathbf{S} \rangle \cdot \tilde{\mathbf{A}} \cdot \mathbf{T}$ in eq 2, is quite sizable. When the external field is increased to 25 kG the magnetic splitting reflects the increased values of $\langle \mathbf{S} \rangle$ and becomes the dominant factor in the determination of the overall spectrum (Figure 5). At 25 kG the internal magnetic field is saturated; i.e., $\langle \mathbf{S} \rangle$ has almost reached its maximum value and any further increase of the applied field results in a reduction of the magnetic splitting (the applied field opposes the internal field, see eq 3; both $\tilde{\mathbf{A}}$ and $\langle \mathbf{S} \rangle$ have negative values).

As a first step in our analysis we discuss how the zero-field splitting parameters can be extracted from the spectra. Notice that the magnetic splitting does not increase appreciably (less than 7%) when the temperature is lowered from 4.2 to 1.6 K (Figure 3). Hence it follows that only the ground singlet of the spin quintet is appreciably populated at 4.2 K (see eq 4). This observation places a lower limit on the magnitude of the zero-field splitting, $D > 15$ K. To obtain a quantitative estimate of the zero-field splitting parameters we have calculated the temperature dependence of the components of $\langle \mathbf{S} \rangle_T$ from eq 1 as a function of $D$ and $E/D$ in the fast relaxation limit.[1] Since the experimentally observed magnetic splitting not only depends on $\langle \mathbf{S} \rangle_T$, but

[1] An attempt was made to simulate the spectra of Figure 3 in the slow relaxation limit. At 1.6 and 4.2 K only the lowest spin singlet is occupied, and the simulations for fast and slow relaxation are practically indistinguishable. For higher temperatures, however, the predictions based on the two limiting cases differ considerably. For fast relaxation the peaks are flat-topped and narrow as shown in Figure 3. For slow relaxation, on the other hand, the peaks assume a triangular shape and are very broad. Apparently neither of the two limiting cases adequately reproduces the data, and there is reason to believe that an intermediate relaxation model should be used. No attempt was made to develop such a model, since the simulations based on the fast relaxation limit were deemed adequate for the present purpose, i.e., the determination of $D$ and $E$. If the spin relaxation rate is indeed intermediate at $T \sim 10$ K and $\mathbf{H} = 6.6$ kG, then the 4.2 K spectra of Figures 4 and 5 might be close to the slow relaxation limit. For reasons stated above the simulations of the 4.2 K data are insensitive to the assumed relaxation rate and no direct evidence about its magnitude can be derived. Although the theoretical spectra of Figures 3–5 and 8 were calculated in the fast relaxation limit, it should be borne in mind that the only claim made about the relaxation time is that it does not significantly affect the parameters deduced from the data. This statement does not apply to the 180 K spectra of Figure 6 for which the fast relaxation limit undoubtedly applies.

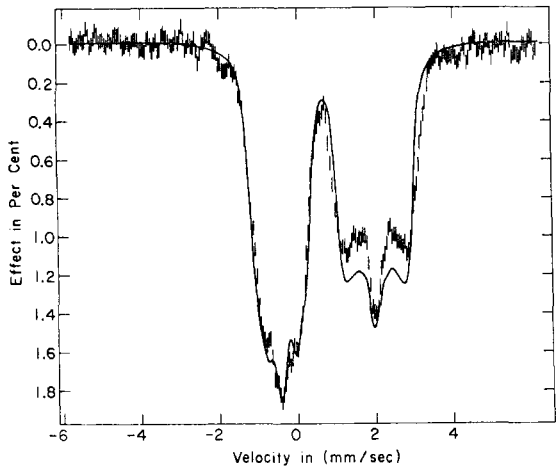


FIGURE 4: Mössbauer spectrum of reduced P-450 taken in a field of 8.6 kG applied parallel to the transmitted $\gamma$ rays at 4.2 K. The solid line is the result of a computer simulation using the parameters listed in Table I and assuming fast relaxation.

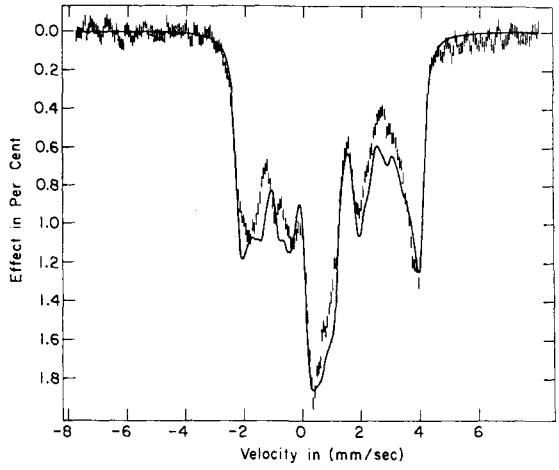


FIGURE 5: Mössbauer spectrum of reduced P-450 taken in a field of 25 kG parallel to the transmitted $\gamma$ rays at 4.2 K. The solid line is the result of a computer simulation using the parameters listed in Table I and assuming fast relaxation.

also on the (poorly known) hyperfine tensor $\tilde{\mathbf{A}}$, the parameters $D$ and $E/D$ cannot be determined separately with good accuracy. However, acceptable ranges appear to be: $D$ = 15 K, $0 \leq E/D \leq 0.1$; or $D$ = 20 K, $0 \leq E/D \leq 0.15$; or $D$ = 25 K and $0 \leq E/D \leq 0.2$. (For a detailed discussion, see Champion, 1975.)

Thus, we have extracted from the Mössbauer spectra the same kind of information that can be obtained from a low-temperature magnetic susceptibility measurement. To obtain an independent determination of the zero-field splitting parameters we have used the latter technique in collaboration with Dr. T. H. Moss of the IBM Watson Laboratory. The susceptibility experiments indicate values of $D$ that are greater than 15 K but less than 25 K although the accuracy is not sufficient to allow a precise determination of $D$ and $E/D$ (Champion et al., 1975a). The agreement between the two methods is encouraging; it shows that low-field, variable temperature Mössbauer experiments are a useful alternative to magnetic susceptibility measurements.

The spectra in Figures 3 and 4 yield crucial information about the orientation of the electric-field gradient tensor (EFG tensor). For $D > 0$ the solutions to eq 1, at low temperatures, always yield $\langle S_z \rangle_T \approx 0$, i.e., the internal magnetic field is essentially in the x-y plane of the zero-field splitting. (This plane is not necessarily coincident with the heme plane; information relating the various interactions to molecular geometry can only be obtained from measurements of single crystals.) If the largest component of the EFG tensor ($V_{\zeta\zeta}$) were oriented along the $z$ axis, the spectra in Figures 3 and 4 would have quite different absorption features; one absorption band would be much broader than the other one (see the low-field spectrum of ferrous fluorosilicate in Figure 2a of Spiering et al., 1974). The spectral features in Figures 3 and 4 can only be explained by assuming that the two largest components of the EFG tensor are close to the $x$-$y$ plane, i.e., $V_{\zeta\zeta}$ is substantially tilted away from the $z$ axis defining the zero-field splitting. The recognition of this rotation turned out to be crucial for the successful simulation of the spectra shown in Figures 3-5.

As mentioned above, the electronic spin moments will begin to obey the Curie law when the temperature is large compared to the energy separation of the five spin states. Thus at infinite temperature, $\langle \mathbf{S} \rangle_T \approx 0$, and the paramagnetic contribution to the Mössbauer spectrum vanishes so

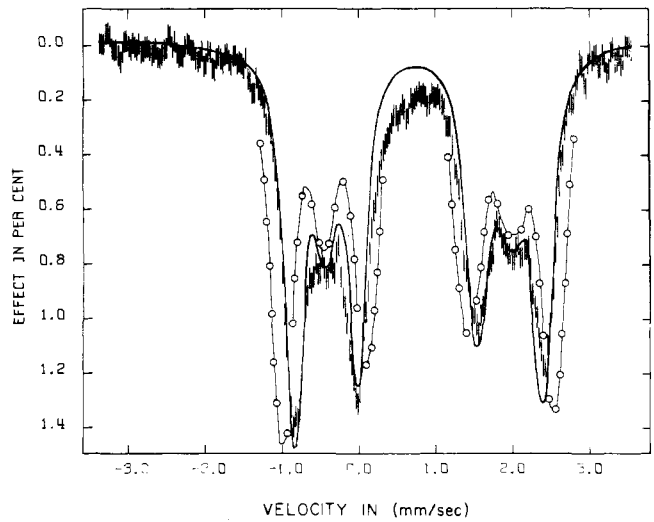


FIGURE 6: Mössbauer spectrum of P-450 taken in a 45-kG parallel magnetic field at 180 K. The solid line is a simulation based on the parameters listed in Table I assuming fast relaxation. The circled line represents a simulation utilizing the same parameters, but assumes pure diamagnetism, i.e., $\langle \mathbf{S} \rangle_T \cdot \tilde{\mathbf{A}} \cdot \mathbf{I} = 0$. The data clearly show effects due to the magnetic hyperfine interaction.

that only the quadrupole and nuclear Zeeman terms in eq 3 remain. Hence the sample behaves like a diamagnetic compound at higher temperature. Under these conditions we can determine $\eta$, the asymmetry parameter, and the sign of $V_{\zeta\zeta}$. Figure 6 shows a Mössbauer spectrum of reduced P-450, taken at 180 K in a field of 45 kG applied parallel to the observed $\gamma$ rays. Using a computer program (Münck et al., 1973) we have simulated a theoretical Mössbauer spectrum assuming $\langle \mathbf{S} \rangle_T = 0$. The solid line connecting the circles in Figure 6 shows the result. The difference between the overall splitting of the theoretical curve and the experiment is due to a residual hyperfine field, $\mathbf{H}_{int} = -\langle \mathbf{S} \rangle_T \cdot \tilde{\mathbf{A}} / \mathbf{g}_n \beta_n$. (At 180 K the components of $\langle \mathbf{S} \rangle_T$ are between 0.06 and 0.09 for $D$ = 15 K.)

The spectrum in Figure 6 may be compared with a high-field spectrum of a true diamagnet, the low-spin ferrous ($S$ = 0) CO adduct of reduced P-450. Figure 7 shows the spectrum of this complex taken at 4.2 K in a 25.5-kG parallel

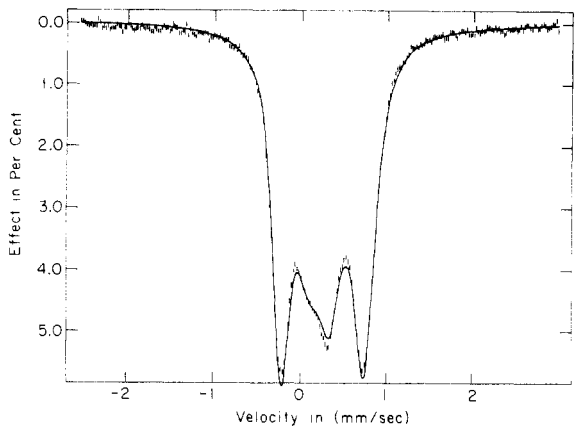


FIGURE 7: Mössbauer spectrum of the carbon monoxide complex of P-450 taken at 4.2 K in a 25.5-kG parallel field. The solid line is a computer simulated spectrum using the following set of parameters: $\Delta E_Q = +0.29$ mm/sec, $\eta = 0.5$, and $\Gamma = 0.25$ mm/sec. The agreement between theory and experiment is not perfect; the sample contains a few percent of high-spin ferrous iron contamination, and thickness broadening was not taken into account. However, $\eta$ can be determined to $\eta = 0.5 \pm 0.2$.

field. The solid line is a theoretical fit using[2] $\mathbf{H}_{int} = 0$ and the parameters listed in the figure caption.

It is clear that a detailed fit to the spectrum shown in Figure 6 requires some knowledge about the magnetic hyperfine tensor $\tilde{\mathbf{A}}$. However, dozens of computer simulations have convinced us that we can estimate $\eta$ fairly well; the spectrum shown in Figure 6 is not compatible with values of $\eta$ less than 0.6, as long as we keep the components of the $\mathbf{A}$ tensor within reasonable bounds.

Up to this point we have restricted ourselves to a procedure by which we estimate some important parameters by mere inspection of the data coupled with some computer simulations. Once we have reasonable estimates for $D$, $E$ and $\eta$, and know the orientation of the EFG tensor, the task of solving the multiparameter problem is greatly facilitated. To further reduce the parameter space to be searched we can restrict the $x$ and $y$ components of the $\mathbf{A}$ tensor to the values $-200$ kG $< \mathbf{A}_i/\mathbf{g}_g\beta_n < -100$ kG.[3] Another simplification arises if we ignore the fact that the principal axes system of the $\mathbf{A}$ tensor need not coincide with the frame defined by the zero-field splitting. This can be done without much loss of generality because it is really the quantity $\mathbf{H}_{int} \propto \langle \mathbf{S} \rangle_T \cdot \tilde{\mathbf{A}}$ that governs the Mössbauer spectrum, and the three components of the $\mathbf{A}$ tensor, diagonal in the principal axes system of the zero-field splitting, can still yield a very general $\mathbf{H}_{int}$. In addition, model calculations (Champion, 1975) have shown that, even in low symmetries, the off-diagonal elements of $\tilde{\mathbf{A}}$ are usually quite small when expressed in the electronic principal axes system.

Table I: Parameters Used in the Simulation of the Mössbauer Spectra of Reduced Cytochrome P-450.

| | | | |
|---|---|---|---|
| $\Gamma$ | 0.25 mm/sec | $g_x$ | 2.24 |
| $D$ | 20 K | $g_y$ | 2.32 |
| $E/D$ | 0.15 | $g_z$ | 2.00 |
| $V_{zz}$ | Positive | | |
| $\Delta E_Q$ | (+)2.42 mm/sec | Euler Angles Taking $\tilde{\mathbf{D}}$ into EFG | |
| $\eta$ | 0.8 | $\alpha_{efg}$ | 60° |
| $A_x'$ | −180 kG | $\beta_{efg}$ | 70° |
| $A_y'$ | −125 kG | $\gamma_{efg}$ | 0° |
| $A_z'$ | −150 kG | | |
| | | Euler Angles Taking $\tilde{\mathbf{D}}$ into $\tilde{\mathbf{A}}$ | |
| | | $\alpha_A$ | 0° |
| | | $\beta_A$ | 0° |
| | | $\gamma_A$ | 0° |

The next and final steps of the data analysis involve spectral simulations with a computer program[4] that generates Mössbauer spectra for polycrystalline specimens from eq 1 and 2. By choosing initial parameters as they have emerged from the inspection procedure we were able to simulate spectra which represent the overall shape of the experimental data quite well. It is absolutely necessary to tilt the EFG tensor away from the $z$ axis of the zero-field splitting tensor; we were unable to obtain simulations resembling the spectrum shown in Figure 5 when we kept $V_{\zeta\zeta}$ aligned with the electronic $z$ axis. A final set of parameters was found by employing an iteration procedure: after many refinements of single spectra the parameters were cross-checked against the entire set of experimental spectra. The solutions thus obtained reflect a set of parameters consistent with the spectra obtained under various experimental conditions. The solid curves through the data points in Figures 3–6 represent the best set of parameters we have obtained after simulating hundreds of spectra; the parameters used to generate these curves are quoted in Table I. The most surprising result of the simulations is the fact that the EFG tensor is rotated substantially away ($\beta = 70°$) from the $z$ axis of the electronic system. This finding, together with the large value of $\eta$, implies a low symmetry at the heme iron. In an attempt to give the reader some feeling for the dependence of the spectra on the orientation of the field gradient, we have displayed in Figure 8 a set of 25-kG simulations with all parameters, except for $\beta$, identical with those quoted in Table I.

## Discussion

It is instructive to compare the results for reduced P-450 with those obtained for hemoglobin. Although the quadrupole splittings $\Delta E_Q$ of both compounds are quite similar at 4.2 K, a glance at Figure 2 shows that the temperature dependences of $\Delta E_Q$ are quite different. A temperature dependent $\Delta E_Q$ suggests that excited orbital states become populated at higher temperatures. Various theoretical approaches have been pursued to account for the Mössbauer

[2] The Mössbauer parameters of the carbon monoxide complexes of reduced P-450 and of myoglobin (A. Trautwein, to be published in *Struct. Bonding (Berlin)*) are almost indistinguishable; both compounds have a positive quadrupole coupling constant, i.e., $V_{zz} > 0$ ($\eta = 0.5$ for P-450-CO; $\eta$ was not determined for Mb-CO). The similarity of the Mössbauer spectra is quite surprising in view of the drastic differences in the optical absorption spectra of the two proteins. We have to note, however, that the Mössbauer spectra of low-spin ferrous complexes do not give very detailed information; first, they lack magnetic features and second, measurements on polycrystalline materials do not provide information regarding the spatial relation between the field gradient tensor and the molecular axes.

[3] From the spectra of Figures 3 and 4 the $x$ and $y$ components of the internal magnetic field can be estimated, taking into account the rotation of the EFG with respect to the zero-field splitting tensor. Since $\langle \mathbf{S} \rangle_T$ can be calculated from eq 1 and 4 for reasonable values of $D$ and $E$, an estimate of the $x$ and $y$ components of the $\mathbf{A}$ tensor is obtained. Simulations of the spectrum in Figure 6 indicate that the internal field opposes the applied field and, in addition, they limit the components of $\tilde{\mathbf{A}}$ to the values $-200$ kG $\leq \mathbf{A}_i/\mathbf{g}_g\beta_n \leq -100$ kG.

[4] The program used is an extension of a simulation program described earlier (Münck et al., 1973). The modification involves the addition of a subroutine that computes the components of $\langle \mathbf{S} \rangle$ from eq 1.

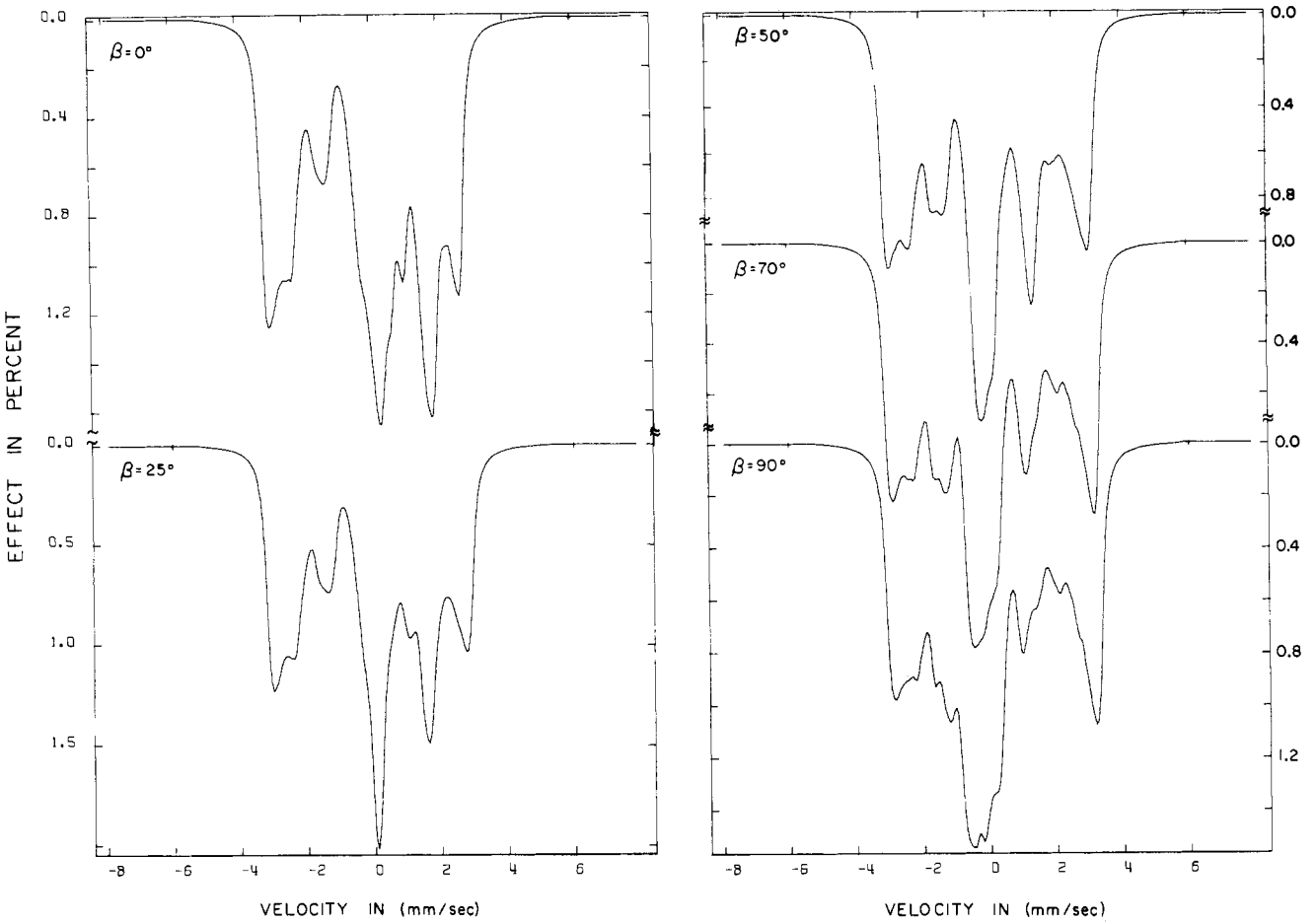


FIGURE 8: A set of theoretical spectra showing how the 25 kG, 4.2 K Mössbauer spectrum varies with $\beta$, the Euler angle relating the $z$ axes of the **D** and EFG tensors. All other parameters are as listed in Table I.

data of hemoglobin and myoglobin. Most recently Huynh et al. (1974) determined the electronic structure of the ferrous ion in hemoglobin using a crystal field approximation that takes into account the entire 210 states of the $3d^6$ configuration. These calculations give good agreement with the Mössbauer data, i.e., the temperature dependence of $\Delta E_Q$ and the orientation of the field gradient relative to the heme plane are accounted for. Moreover, the magnetic susceptibility data of Nakano et al. (1971 and 1972) are well described by the model. For our discussion the results of the calculations on hemoglobin have two interesting aspects: (1) singlet and triplet configurations interpenetrate the ligand-field split $^5D$ term, and (2) the resulting energy levels are spaced such that no isolated spin quintet can be discerned. The fact that the low-temperature susceptibility data can be parametrized in terms of a spin Hamiltonian with $S = 2$ therefore appears fortuitous; the spin Hamiltonian and the crystal field calculations yield drastically different level sequences for the lowest electronic states. Thus, it is unlikely that the zero-field splitting parameters obtained for deoxyhemoglobin ($D = 7.5$ K, $E = 0$; Nakano et al., 1971) can be directly compared to those found for P-450.

A description of the P-450 data in terms of a spin Hamiltonian is probably valid; the temperature independent quadrupole splitting and the successful fits to the paramagnetic Mössbauer spectra support this claim. Therefore we decided to further evaluate the data in the framework of a ligand field model restricting ourselves to the $^5D$ configuration. If the energy separation of the ground and first excited orbital states is large compared to the spin–orbit coupling energy, the spin Hamiltonian parameters can be computed using second-order perturbation theory (Abragam and Bleaney, 1970). From such calculations the properties of the ground state orbital wave function can be deduced. These wave functions reflect the symmetry of the heme iron environment.

Without going into the details of these calculations (Champion, 1975; Champion et al., 1975b) some conclusions can readily be drawn. $D_{2h}$ symmetry (often assumed to apply to the heme iron) will produce a ground state orbital of either $d_{xy}$, $d_{xz}$, or $d_{yz}$ symmetry. Monoclinic ($C_{2h}$), symmetry will produce a mixture of two of these orbitals (Oosterhuis, 1971), while triclinic symmetry ($C_1$) will mix all three orbitals into the ground state.

For orthorhombic symmetry ($D_{2h}$) it is clear that the field gradient of the ground state must have $\eta = 0$.[5] If we take the $d_{xy}$ orbital as an example, it follows from the spatial arrangement of the electronic charge distribution that the electrostatic potential will vary in the same manner along the $x$ and $y$ axis. The situation involving a mixture of two $t_{2g}$ orbitals (monoclinic symmetry) is not so simple, but

[5] This statement is valid only if the admixture of excited orbital states in the orbital ground state can be ignored, i.e., if the excited states are sufficiently far removed in energy from the ground state. Since this condition appears to be satisfied for reduced cytochrome P-450, the analysis of Cosgrove and Collins (1971) applies. Whenever the spin–orbit coupling energy is comparable with the splittings produced by lower symmetry components of the ligand field, however, this simple treatment is not adequate as was pointed out by Dale (1972).

it has been treated along with the more general case (a mixture of all three orbitals) by Cosgrove and Collins (1971). It turns out that $\eta$ vanishes even in monoclinic symmetry, and triclinic symmetry is required in order to mix all three wave functions, thus generating non-zero values of $\eta$.

With this in mind our experimental determination of $0.6 < \eta < 1.0$ implies a very low symmetry[6] (triclinic) at the heme iron of reduced cytochrome P-450. Moreover, the fact that the principal axes of the field gradient and zero-field splitting tensors do not coincide is further evidence for a low symmetry, since in orthorhombic or higher symmetry all tensors must be aligned.

Thus, we have seen that the intricate Mössbauer spectra of heme proteins in the high-spin ferrous state provide a wealth of information. Cytochrome P-450 is the first protein for which a detailed analysis of the data has been achieved. It is clear that this is just a beginning. The Mössbauer effect will certainly be used further as a tool for the elucidation of the structural details of high-spin ferrous heme proteins. It is promising that zero-field splitting parameters can be determined quite well with this technique. As a result, Mössbauer spectroscopy can substitute for magnetic susceptibility measurements when the latter method cannot be applied because of the presence of paramagnetic impurities (chloroperoxidase, discussed in the following paper, is an example). Moreover, the Mössbauer effect provides the means of probing the symmetry of the active site.

The biochemical information that can be straightforwardly extracted from a spectroscopic investigation relies heavily on the comparison of the data with those obtained from compounds with a known structure. In the following paper we will extend our discussion by comparing the Mössbauer results for P-450 with results obtained for hemoglobin, chloroperoxidase, and horseradish peroxidase.

References


Abragam, A., and Bleaney, B. (1970), in Electron Paramagnetic Resonance of Transition Ions, London, Oxford University Press.

Bayer, E., Hill, H. A. O., Röder, A., and Williams, R. J. P. (1969), *Chem. Commun.*, 109.

Champion, P. M. (1975), Ph.D. Thesis, University of Illinois.

Champion, P. M., Chiang, R., Münck, E., Debrunner, P., and Hager, L. P. (1975c), *Biochemistry*, following paper in this issue.

Champion, P. M., Münck, E., and Debrunner, P. G. (1975b), *J. Chem. Phys.*, submitted for publication.

Champion, P. M., Münck, E., Debrunner, P. G., Moss, T., Lipscomb, J., and Gunsalus, I. C. (1975a), *Biochim. Biophys. Acta 376*, 579.

Cosgrove, J., and Collins, R. (1971), *J. Chem. Phys. 55*, 4238.

Dale, B. W. (1972), *J. Chem. Phys. 56*, 4721.

Garfinkel, D. (1958), *Arch. Biochem. Biophys. 77*, 493.

Gunsalus, I. C., Meeks, J. R., Lipscomb, J. D., Debrunner, P., and Münck, E. (1974), in Molecular Mechanisms of Oxygen Activation, Hayaishi, O., Ed., New York, N.Y., Academic Press, p 559.

Hedegaard, J., and Gunsalus, I. C. (1965), *J. Biol. Chem. 240*, 4038.

Huynh, B. H., Papaefthymiou, G., Yen, C. S., Groves, J. L., and Wu, C. S. (1974), *J. Chem. Phys. 61*, 3750.

Imai, Y., and Sato, R. (1974), *Biochem. Biophys. Res. Commun. 60*, 8.

Johnson, C. E. (1967), *Proc. Phys. Soc. 92*, 748.

Klingenberg, M. (1958), *Arch. Biochem. Biophys. 75*, 376.

Münck, E., Groves, J. L., Tumolillo, T., and Debrunner, P. G. (1973), *Comput. Phys. Commun. 5*, 225.

Nakano, N., Otsuka, J., and Tasaki, A. (1971), *Biochim. Biophys. Acta 236*, 222.

Nakano, N., Otsuka, J., and Tasaki, A. (1972), *Biochim. Biophys. Acta 278*, 355.

Oosterhuis, W. (1971), *Phys. Rev. 3*, 546.

Schleyer, H., Cooper, D. Y., Levin, S. S., and Rosenthal, O. (1972), in Biological Hydroxylation Mechanisms, Boyd, G. S., and Smellie, R. M. S., Ed., New York, N.Y., Academic Press, p 187.

Sharrock, M., Debrunner, P. G., Schulz, C., Lipscomb, J. D., Marshall, V., and Gunsalus, I. C. (1975), *Biochim. Biophys. Acta*, submitted for publication.

Sharrock, M., Münck, E., Debrunner, P., Marshall, V., Lipscomb, J., and Gunsalus, I. C. (1973), *Biochemistry 12*, 258.

Spiering, H., Zimmerman, R., and Ritter, G. (1974), *Phys. Status Solidi B, 62*, 123.

Stern, J., and Peisach, J. (1974), *J. Biol. Chem. 249*, 7495.

Stern, J. O., Peisach, J., Blumberg, W. E., Lu, A. Y. H., and Levin, W. (1973), *Arch. Biochem. Biophys. 156*, 404.

Trautwein, A., Eicher, H., and Mayer, A. (1970), *J. Chem. Phys. 52*, 2473.

Van der Hoeven, T. A., Haugen, D. A., and Coon, M. J. (1974), *Biochem. Biophys. Res. Commun. 60*, 569.

Zimmermann, R., Spiering, H., and Ritter, G. (1974), *Chem. Phys. 4*, 133.


[6] Our crystal field calculations involve parameters describing an octahedral field with tetragonal and rhombic distortions (spin–orbit coupling included) acting on the $^5D$ configuration. To account for the low symmetry components, the tetragonal and rhombic distortions were allowed to have arbitrary orientations relative to the octahedral field. A computer program was used to search the parameter space for solutions that produce a temperature independent $\Delta E_Q$ and values of $D$ and $\eta$ within their experimental tolerances. After this screening process the parameters were refined. The best set of crystal field parameters yields $D = 23.5$ K, $E/D = 0.12$, $\eta = 0.99$, and, most importantly, a reasonably accurate orientation of the field-gradient tensor. All three $t_{2g}$ orbitals contribute sizably to the wave function of the orbital ground state. The first excited orbital state is placed 980 K above the ground state. Details of these calculations are described elsewhere (Champion, 1975; Champion et al., 1975b).